

Universal scheme for integrating cold atoms into optical waveguides

Elisa Da Ros,¹ Nathan Cooper,¹ Jonathan Nute,¹ and Lucia Hackermueller¹

School of Physics and Astronomy, University of Nottingham, Nottingham, NG7 2RD, United Kingdom^{a)}

(Dated: 7 October 2022)

Hybrid quantum devices, incorporating both atoms and photons, can exploit the benefits of both to enable scalable architectures for quantum computing and quantum communication, as well as chip-scale sensors and single-photon sources. Production of such devices depends on the development of an interface between their atomic and photonic components. This should be compact, robust and compatible with existing technologies from both fields. Here we demonstrate such an interface. Cold caesium atoms are trapped inside a transverse, $30\ \mu\text{m}$ diameter through-hole in an optical fibre, created via laser micromachining. When the guided light is on resonance with the caesium D_2 line, up to 87% of it is absorbed by the atoms. The corresponding optical depth per unit length is $700\ \text{cm}^{-1}$, higher than any reported for a comparable system. This is important for miniaturisation and scalability. The technique should be equally effective in optical waveguide chips and other existing photonic systems.

I. INTRODUCTION

Interfacing cold atoms with optical waveguides has been a very active field of research over the past two decades^{1–7}. This has been motivated by the great potential of hybrid atom-photon systems for sensing, quantum communication and quantum information processing^{2,8–10}. Existing approaches tend to involve purpose designed systems such as tapered nanofibres^{11–15}, hollow-core fibres^{16–20} or other custom-built waveguide and photonic crystal structures^{21,22}, which don't lend themselves readily to integration. Herein we describe a universal technique, capable of interfacing cold atoms with nearly any existing waveguide system. This new approach will allow hybrid devices to take full advantage of the capabilities of all-optical waveguide chips, which have reached a very high level of development^{23–25}. The increased range and complexity of operations thus permitted can be expected to greatly expand the potential of hybrid atom-photon devices, opening the door to long-standing experimental and technological goals^{1,2,8,9}.

The basis of the technique described herein is the introduction of cold atoms into microscopic, laser-drilled holes in optical waveguides, see Fig. 1a and 1b. Laser micromachining can be used to create holes at any desired location(s) within a very wide range of materials, including most glasses and ceramics, silicon, metals and polymers²⁶. This is a significant advantage over techniques linked to specific waveguide materials and architectures, as it will allow the method to be applied easily across a broad range of waveguide devices and to take full advantage of advances in subwavelength integrated optics and optical metamaterials²⁷. Furthermore, the shape of these holes can be controlled and modified according to the needs of the user²⁸, see Fig 1c.

Drilling a transverse hole through an optical waveguide allows cold atoms to be directly overlapped with the centre of the propagating mode of the waveguide and hence enables good coupling between photons and atoms. It has been shown that with the addition of an optical

cavity strong coupling between the atoms and the guided light should be achievable in such systems²⁸. The technique should be extendible to multiple holes in a single waveguide, thus allowing atoms at different sites to be coherently coupled via the optical field.

We provide an experimental demonstration of the above technique within a standard, single-mode optical fibre (Thorlabs 780HP). A cloud of cold Cs atoms is guided into $30\ \mu\text{m}$ diameter cylindrical through-hole, drilled orthogonally to the core of the fibre. The atoms absorb 87% of the optical power of a resonant probe beam travelling through the fibre.

The small size of the interaction region, which is some tens of micrometres in length, is a clear advantage over existing methods, e.g. many fibre-based experiments involve interaction regions with lengths on the centimetre scale. We measure the optical depth per unit length of our trapped atom cloud at $700\ \text{cm}^{-1}$, greater than any value found in the literature for a comparable system^{29,30}. This has important benefits for device miniaturisation, enabling scalability of the number of waveguide-atom interfaces within a small device and improving spatial resolution in sensing applications⁸. In the directions transverse to the propagation axis, the interface retains the small mode area of the waveguide. The tight confinement of the light while traversing the interaction region naturally helps to achieve strong atom-photon coupling^{17,31}.

The technique permits large atom-surface separations. This diminishes the influence of decoherence and line-broadening effects caused by atom-surface interactions, enabling the use of charged or highly polarisable particles. Rydberg atoms are an important example of such polarisable particles, with significant applications for sensing and multi-qubit atomic gate operations^{32,33}.

Furthermore, the ability to hold the atoms within the interaction region for a prolonged period using an optical dipole trap allows sequential or time-separated operations.

Overall, the approach described herein results in a compact, robust interface that can be directly inserted wherever it is needed within an existing waveguide architecture. Our results represent an important advance towards the goal of combining cold atoms and optical waveguides into an integrated and scalable quantum device.

^{a)}nathan.cooper@nottingham.ac.uk

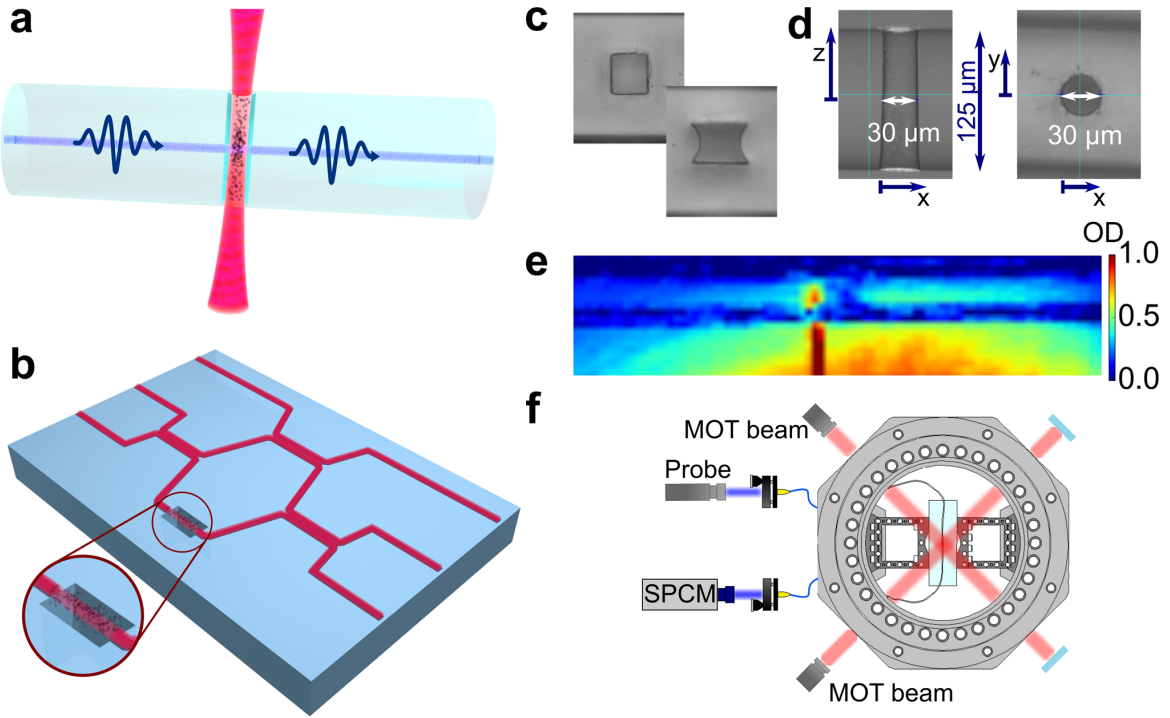


Fig. 1. **a**, Illustration of an atom cloud confined within a microscopic hole in an optical fibre using an optical dipole trap (red beam) and interfaced with light guided in the fibre (blue beam). **b**, Illustration showing the proposed use of this technique for the inclusion of cold atoms in a waveguide chip. **c** and **d**, Examples of differently shaped laser drilled holes and side and top view of the hole used in this study, images by Workshop of Photonics. **e**, Absorption image of caesium atoms confined in an optical dipole trap aligned with the void in the fibre (fibre visible as a horizontal feature at the centre of the image). **f**, Schematic of the setup (top view). Atoms are trapped in a magneto-optical trap below the interface, then guided to the interaction region via an optical dipole trap. Here they are probed by light propagating in the fibre (blue beam). The output is collected by a single photon counting module.

II. RESULTS

Our experimental setup is illustrated in Fig. 1. The interface is based on a commercially available single mode optical fibre with a mode field diameter of $(5.0 \pm 0.5) \mu\text{m}$ at 850 nm and a cladding diameter of 125 μm . The fibre has been laser drilled with a cylindrical through hole perpendicular to the light propagation axis, with diameter $D = 30 \mu\text{m}$, as shown in Fig. 1d. Laser drilling was performed by Workshop of Photonics.

For mounting purposes, the fibre is attached to a glass slide, which is then placed into a vacuum chamber. The fibre enters the vacuum system through custom built fibre-feedthroughs³⁴ and the region containing the hole is suspended in the centre of the vacuum chamber. Approximately 3×10^7 ^{133}Cs atoms are loaded into a magneto-optical trap (MOT), about 1 mm below the fibre. To cool the cloud further, the trapping lasers are then detuned by 13Γ in an 18 ms optical molasses stage (where Γ is the natural linewidth of the transition). During this time the atoms are also optically pumped to the $\{6^2S_{1/2}, F = 4\}$ state. At the same time the magnetic field gradient used to generate the MOT is ramped down and the magnetic field centre is displaced upwards by increasing an offset field. This transport technique allows us to achieve an atom density $n \approx 5 \times 10^{10} \text{ atoms/cm}^3$ immediately below the hole in the fibre.

A fibre laser with a wavelength of 1064 nm and a

maximum power of 25 W is used to create an optical dipole trap for the atoms. The trap consists of a vertical beam which is focused down to a waist of 13 μm and aligned through the hole in the optical fibre, see Fig. 1e. The focal point lies within the interaction region. After switch-off of the MOT beams, a hold-time of 3 ms allows the atoms to migrate along the dipole trap beam into the interaction region.

Pulses of probe light are sent through the fibre so that they interact with the atoms. For this we use light resonant with the $|g\rangle = \{6^2S_{1/2}, F = 4\} \rightarrow |e\rangle = \{6^2P_{3/2}, F = 5\}$ transition of ^{133}Cs . One microsecond before the probing pulse, the dipole trapping beam is switched off. The output of the optical fibre is directed onto a single photon counting module (SPCM), as shown in Fig. 1f, which is used to determine the number of transmitted photons.

In order to measure the fraction of the probe light absorbed by the atom cloud, we count the number of photons received during a 15 μs probe beam pulse. We then repeat the measurement after a 100 ms delay, during which the atoms are dispersed. The absorption fraction is determined from the ratio of the two results. In order to avoid saturating the atomic transition, very low probe beam powers (on the order of pW) are necessary, and as a result photon counting statistics become our dominant source of experimental random error, see Methods. We average multiple measurements (typically between 30 and

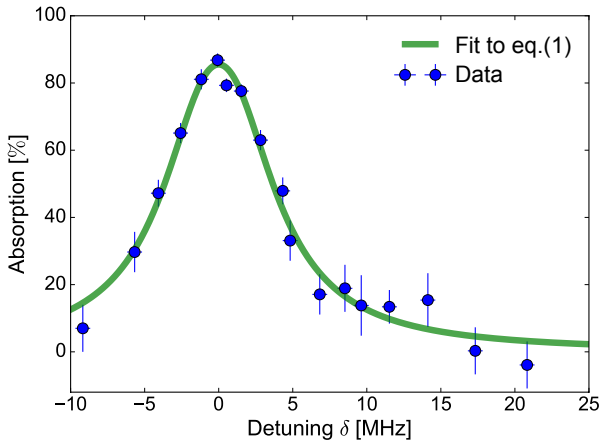


Fig. 2. Fractional absorption of the probe beam light by the atoms as a function of the detuning δ from the $|g\rangle = \{6^2S_{1/2}, F = 4\} \rightarrow |e\rangle = \{6^2P_{3/2}, F = 5\}$ ^{133}Cs transition. Each point corresponds to the mean of 36 repetitions, with the error bars representing the standard deviation. The solid line is a fit according to eq. (1).

100) for any given set of experimental conditions, thus reducing the statistical uncertainty.

Using a probe beam power $P_{\text{pr}} = 13$ pW, we measured $(87 \pm 2)\%$ absorption caused by the atoms, corresponding to an optical depth (OD) of 2.1 ± 0.2 , leading to an optical depth per unit length of 700 cm^{-1} . This implies the presence of 290 ± 20 Cs atoms in a volume of $600 \mu\text{m}^3$ and corresponds to an average density on the order of $5 \times 10^{11} \text{ atoms/cm}^3$, assuming a uniform atomic distribution across the interaction region. These values therefore represent a lower limit on the atom number and peak density.

The response of the atomic absorption to changes in probe laser detuning, probe laser power and dipole laser power was measured. Fig. 2 shows the fractional absorption of the probe beam power by the atom cloud as a function of the probe laser detuning δ , as the laser frequency is tuned across the $\{F = 4\} \rightarrow \{F' = 5\}$ transition. The probe beam power was $P_{\text{pr}} = 9$ pW. The resonance profile derives from the natural linewidth of the atomic transition Γ , with the atomic absorption response in percent given by¹⁷

$$\text{Abs} = 100 \left(1 - \exp \left(\frac{-\text{OD}}{1 + 4(\frac{\delta}{\Gamma})^2} \right) \right). \quad (1)$$

This model is valid in the limit of low atomic saturation (i.e. the intensity of the probe light, I , must be very much lower than the saturation intensity, I_{sat} of the atomic transition), which is fulfilled in this case. The green line in Fig. 2 represents a fit of equation (1) to the experimental data, where natural linewidth and optical depth have been used as free parameters. This fit results in values of $\text{OD} = 1.9 \pm 0.2$ and $\Gamma = 2\pi \times (5.5 \pm 0.4)$ MHz. The experimentally derived value for Γ is in good agreement with the theoretical value of $2\pi \times 5.2$ MHz, proving that the atomic transition is not noticeably broadened by the presence of the fibre.

The dependence of the atomic absorption response on the probe beam power was characterised and the results are shown in Fig. 3. The fact that, in this case, neither the optical depth nor the ratio of the probe beam intensity to the atomic saturation intensity can be approximated as small necessitates a numerical approach to modelling this situation.

Consider an element of the incident intensity distribution at a specific position $I(0, y, z)$. Employing the standard assumption of direct ray propagation^{35,36}, the intensity I of the light traversing the atom cloud will obey the differential equation

$$\frac{dI(x, y, z)}{dx} = -n\sigma_0 \frac{I(x, y, z)}{1 + \frac{I(x, y, z)}{I_{\text{sat}}}}. \quad (2)$$

where n represents the mean atomic density in the interaction region and σ_0 represents the atomic absorption cross section on resonance. The atomic density can be approximated as uniform along the y and z directions, see Methods. The distribution of the atoms along the x axis, while non-uniform, does not affect the final light intensity resulting from our model. We solve equation (2) numerically for $I(D, y, z)$, the probe light intensity transmitted through the hole at position (y, z) , where the incident optical intensity $I(0, y, z)$ is given by the input power P and the mode profile of the fibre. We assume that, in the z axis as shown in Fig. 1d, the propagating light mode of the fibre is not significantly altered as it traverses the junction. In the y axis, the curvature of the hole acts as a cylindrical lens, leading to a divergence of the propagating beam mode. To account for this we use a simplistic model, where it is assumed that light incident too far from the fibre axis, at coordinates with $|y|$ greater than a cut-off distance c_y , will not be coupled back into the guided mode on the other side of the junction. The cut-off distance c_y is then used as a free parameter when fitting the data to the model.

Integrating over the dimensions (y, z) then results in the total absorption:

$$\text{Abs} = 1 - \frac{1}{P} \int_{-c_z}^{c_z} \int_{-c_y}^{c_y} I(D, y, z) dy dz, \quad (3)$$

where P is the total power within the integration area

$$P = \int_{-c_z}^{c_z} \int_{-c_y}^{c_y} I(0, y, z) dy dz, \quad (4)$$

c_z is taken to be large compared to the mode radius of the fibre, and $I(0, y, z)$ takes into account the Gaussian distribution of the probe beam intensity.

Fitting the data to this model, with the atom density n and the y cut-off distance c_y as free parameters, gives the theoretical fit plotted in Fig. 3. The resulting value $c_y = (1.9 \pm 0.3) \mu\text{m}$ is comparable to the fibre mode radius, as expected. The corresponding atom density $n \approx (2.9 \pm 0.1) \times 10^{11} \text{ atoms/cm}^3$ implies the presence of 170 ± 5 atoms in the interaction region. We assume that the light reaching the atoms is linearly polarised, and use the corresponding saturation intensity

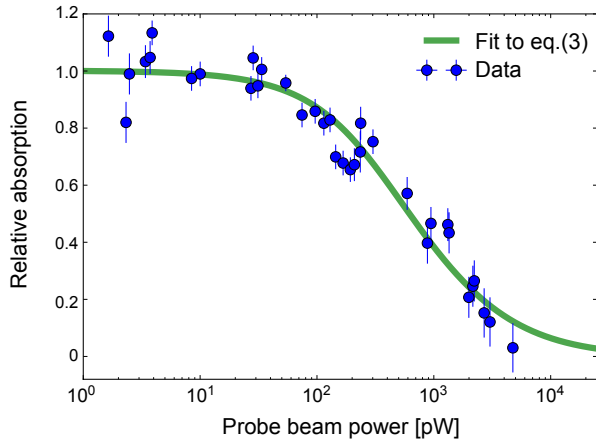


Fig. 3. Relative absorption of resonant probe light as a function of the incident probe beam power. Each point corresponds to the mean of 49 repetitions, with the error bars representing the standard deviation. The solid line is a fit according to eq. (3).

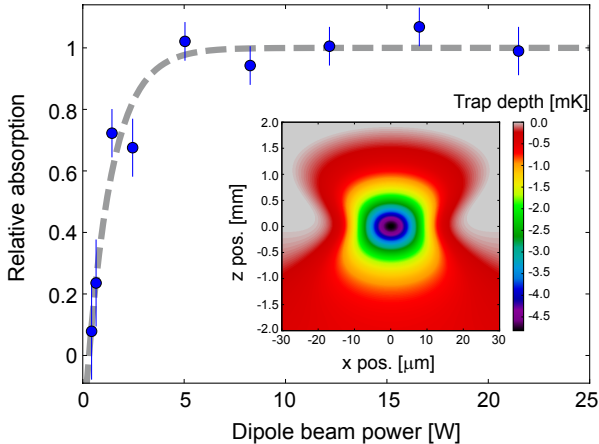


Fig. 4. Relative absorption of resonant probe light as a function of the power in the optical dipole trapping beam. Each point corresponds to the mean of 49 repetitions, with the error bars representing the standard deviation. The line plot is a purely empirical guide to the eye. In the inset the trapping potential is depicted for 5 W of trapping power. The asymmetry in the plot is due to gravity.

$I_{\text{sat}} = 1.66 \text{ mW/cm}^2$, although small deviations from this are possible as the fibre is not polarisation maintaining. Finally, the absorption of the probe beam was measured as a function of the power used in the dipole trapping beam, as shown in Fig. 4. The results show that, for powers in excess of 5 W (corresponding to trapping frequencies of $\nu_r \approx 76 \text{ KHz}$ in the radial direction and $\nu_z \approx 2.0 \text{ KHz}$ in the longitudinal direction), the number of atoms loaded into the interaction region is no longer limited by the power of the dipole trapping beam. This indicates that for powers larger than 5 W the depth of the optical dipole trap has become large compared to the temperature of the atomic cloud. The fact that the probe absorption appears to drop to zero for finite dipole beam powers is expected given the influence of gravity on the trapping potential.

III. CONCLUSIONS AND OUTLOOK

We have demonstrated efficient coupling of cold atoms, introduced into a laser-micromachined hole in an optical waveguide, to the light guided in the waveguide. This method for interfacing atoms and waveguides is applicable within a wide range of waveguide architectures and offers high optical depth per unit length. It will have important applications in the production of miniaturised atom-optical devices for sensing, quantum communication and quantum information processing.

Demonstration of this technique within a more complex waveguide network, together with its use to produce coherent atom-optical effects such as electromagnetically induced transparency³⁷ or four-wave mixing³⁸⁻⁴⁰, represents the next step towards a quantum information processing device based on this architecture.

We have shown in²⁸ that appropriate shaping of the micromachined holes, together with ongoing improvements in fabrication techniques, can greatly reduce the optical losses as light is transmitted across the holes. It is thus conceivable to introduce optical cavities around such holes, for example via the use of laser written Bragg gratings in the waveguides^{41,42}, with a sufficiently high finesse to bring the atom-light system into the strong coupling regime⁴³. For atom numbers comparable to those demonstrated here, we find that cooperativities on the order of $C = 400$ should be possible²⁸. This would enable photonically-mediated interactions between atoms located at distant sites, and also permits single photon gate operations. The technique thus has the potential to directly interface photonic and atomic qubits.

IV. METHODS

Junction details

A commercially available Thorlabs 780HP bare fibre is glued underneath a glass plate, using vacuum compatible UV-cure glue (Dymax Low-Shrink OP-67-LS). A 1 mm diameter, mechanically drilled hole in the glass plate allows unobstructed passage of the dipole and imaging beams through the interaction region. This glass chip is then suspended in the centre of the vacuum chamber, with the central region of the fibre free-hanging for approximately 5 mm. With the current production method we measured 20% transmission efficiency through the hole (without Cs atoms) at 852 nm. Numerical simulations have shown that appropriate shaping of the holes should allow much higher transmission efficiencies²⁸.

Atom loading

The MOT captures around 3×10^7 ^{133}Cs atoms from the background gas within 10 s. The trap forms about 1 mm below the hole in the fibre.

In order to cool the cloud further, the MOT beams are then detuned by $\sim 13 \Gamma$ over 18 ms in a optical molasses stage. At the same time the current flowing in the two coils that generate the magneto-optical trap decreases with unbalanced ramps, modifying the field gradient in the region of the cloud. Simultaneously the magnetic

offset field increases and the cloud is pushed upwards. The presence of the glass plate and the scattering arising from the mechanically drilled hole in the mounting plate adversely affect the MOT beams and hence the MOT loading. The closer the starting position of the trap is to the surface of the chip, the lower the achievable atom density is. The transport stage is therefore necessary to obtain a dense, cold cloud close to the fibre.

The optical dipole trap is switched on 42 ms before the start of the optical molasses stage. The resulting 60 ms of overlap between the dipole trap and the MOT stage was found to maximise the dipole trap loading and the final atom number at the position of the fibre core.

The atoms are assumed to have a uniform distribution in the y and z directions. This is a reasonable assumption in our experiment, as both the Rayleigh length and the waist of the dipole trapping beam substantially exceed the diameter of the probe beam.

Measurement method

Between 1 and 10^4 pW of probe light is coupled into the optical fibre, and the fibre output is then focused onto the photoreceptor of a single photon counting module (Excelitas SPCM-AQRH-14). The number of photons reaching the SPCM is recorded using high frequency binary counter chips connected to an Arduino Uno. A linearity correction function, specified by the manufacturer, is employed to account for the influence of the receptor dead time at high count rates.

In each experimental cycle, two readings are taken from the SPCM: the number of photons received with atoms present in the hole, N_{at} , and the number received without atoms, N_{bgd} . In both cases, the duration of the probe pulse is 15 μ s, with 100 ms allowed between the two pulses for the atoms to disperse.

Unwanted SPCM counts arising from background light sources and scattered dipole trap light are minimised using a laser-line filter (SEMROCK LL01-852), positioned directly in front of the SPCM, and appropriate physical shielding. To compensate for the SPCM dark count rate and residual background light, a control data set is taken without any probe light. The mean number of counts recorded in this condition (~ 1 -2 counts) is then subtracted from all other measurements.

The SPCM sensitivity can be modified following exposure to MOT light during the atom loading stage, and the entire experimental system is subject to small variations that occur repeatedly over the course of an experimental cycle. To account for any systematic bias caused by these effects, the ratio of the counts recorded during the first and second probe pulses is also measured without atoms loaded into the hole, but with probe light in the fibre. To prevent atom loading, the magnetic field used to generate the MOT is switched off, but all other experimental parameters are unchanged. The ratio N_{at}/N_{bgd} that is recorded with atomic loading is then divided by the mean ratio obtained in this condition, such that any remaining systematic difference between N_{at} and N_{bgd} must arise from the presence of the atoms.

The ratio of the two readings N_{at} and N_{bgd} , after these corrections, identifies the transmission of the probe light through the atomic cloud. For statistical purposes each

measurement is averaged over multiple repetitions, typically between 36 and 100.

The optical power incident on the Cs atoms in the hole, P , is estimated from the number of photons recorded by the SPCM without atoms in the hole, N_{bgd} . This estimate takes into account the quantum efficiency of the SPCM, the mode area of the fibre and the optical losses encountered on traversing the hole and subsequent components. It is assumed that loss of light at the hole occurs primarily due to limited coupling back into the guided mode.

REFERENCES

- ¹Duan, L. M. et al. Long-distance quantum communication with atomic ensembles and linear optics. *Nature*, **414**, 413 - 418 (2001).
- ²Kimble, H. J. The quantum internet. *Nature*, **453**, 1023 (2008).
- ³Lepert, G. et al. Arrays of waveguide-coupled optical cavities that interact strongly with atoms. *New J. Phys.*, **13**, 113002 (2011).
- ⁴Thompson, J.D., et al. Coupling a single trapped atom to a nanoscale optical cavity. *Science*, **340**, 6137 (2013).
- ⁵Lee, J., et al. Integrated optical dipole trap for cold neutral atoms with an optical waveguide coupler. *New J. Phys.*, **340**, 6137 (2013).
- ⁶Ritter, R., et al. Coupling thermal atomic vapor to slot waveguides. *Phys. Rev. X*, **8**, 021032 (2018).
- ⁷Hilton, A. P., et al. High-efficiency cold-atom transport into a waveguide trap. *Phys. Rev. Applied*, **10**, 044034 (2018).
- ⁸Monro, T. M., et al. Sensing with microstructured optical fibres. *Meas. Sci. Technol.*, **12**, 854 (2001).
- ⁹Reiserer, A. & Rempe, G. Cavity-based quantum networks with single atoms and optical photons. *Rev. Mod. Phys.*, **87**, 1379 (2015).
- ¹⁰Nieddu, T., Gokhroo, V., & Nic Chormaic, S. Optical nanofibres and neutral atoms. *J. Opt.*, **18**, 053001 (2016).
- ¹¹Sagué, T., et al. Cold-atom physics using ultrathin optical fibers: Light-induced dipole forces and surface interactions. *Phys. Rev. Lett.*, **99**, 163602 (2007).
- ¹²Nayak, K. P., & Hakuta, K. Single atoms on an optical nanofibre. *New. J. Phys.*, **10**, 053003 (2008).
- ¹³Kumar, R., et al. Interaction of laser-cooled 87Rb atoms with higher order modes of an optical nanofibre. *New. J. Phys.*, **17**, 013026 (2015).
- ¹⁴Patterson, P., et al. Spectral Asymmetry of Atoms in the Van der Waals Potential of an Optical Nanofiber. *Phys. Rev. A*, **97**, 032509 (2018).
- ¹⁵Corzo, N. V., et al. Waveguide-coupled single collective excitation of atomic arrays. *Nature*, **566**, 359-362 (2019).
- ¹⁶Renn, M. J., et al. Laser-guided atoms in hollow-core optical fibers. *Phys. Rev. Lett.*, **75**, 3253 (1995).
- ¹⁷Bajcsy, M., et al. Efficient all-optical switching using slow light within a hollow fiber. *Phys. Rev. Lett.*, **102**, 203902 (2009).
- ¹⁸Okaba, S., et al. Lamb-Dicke spectroscopy of atoms in a hollow-core photonic crystal fibre. *Nat. Comm.*, **5**, 4096 (2014).
- ¹⁹Blatt, F., et al. Stationary light pulses and narrowband light storage in a laser-cooled ensemble loaded into a hollow-core fiber. *Phys. Rev. A*, **94**, 043833 (2016).
- ²⁰Langbecker, M., et al. Highly controlled optical transport of cold atoms into a hollow-core fiber. *New. J. Phys.*, **20**, 083038 (2018).
- ²¹Kohnen, M., et al. An array of integrated atom-photon junctions. *Nat. Photonics*, **5**, 35 (2010).
- ²²Hood, J. D., et al. Atom-atom interactions around the band edge of a photonic crystal waveguide. *PNAS*, **113**, 10507 (2016).
- ²³Marshall, G. D., et al. Laser written waveguide photonic quantum circuits. *Opt. Express*, **17**, 12546 (2009).
- ²⁴Sansoni, L., et al. Polarization entangled state measurement on a chip. *Phys. Rev. Lett.*, **105**, 200503 (2010).
- ²⁵Poulios, K., et al. Quantum walks of correlated photon pairs in two-dimensional waveguide arrays. *Phys. Rev. Lett.*, **112**, 143604 (2014).

²⁶Mishra, S., & Yadava, V. Laser beam micromachining (LBMM) a review. *Opt. Lasers Eng.*, **73**, 122 (2015).

²⁷Cheben, P., et al. Subwavelength integrated photonics. *Nature*, **560**, 7220 (2018).

²⁸Cooper, N., et al. Prospects for strongly coupled atom-photon quantum nodes. *Sci. Rep.*, in print (2019), arXiv:1812.06020.

²⁹Kaczmarek, K. T., et al. Ultrahigh and persistent optical depths of cesium in kagomé-type hollow-core photonic crystal fibers. *Opt. Lett.*, **40**, 5582 (2015).

³⁰Dawkins, S. T., et al. Dispersive optical interface based on nanofiber-trapped atoms. *Phys. Rev. Lett.*, **107**, 243601 (2011).

³¹Tey, M. K., et al. Strong interaction between light and a single trapped atom without the need for a cavity. *Nat. Phys.*, **4**, 924 (2008).

³²Urban, E., et al. Observation of Rydberg blockade between two atoms. *Nat. Phys.*, **5**, 110 (2009).

³³Petrosyan, D., et al. High-fidelity Rydberg quantum gate via a two-atom dark state. *Phys. Rev. A*, **96**, 042306 (2017).

³⁴Abraham, E. R. I., et al. Teflon feedthrough for coupling optical fibers into ultrahigh vacuum systems. *Appl. Opt.*, **37**, 1762 (1998).

³⁵Goban, A., et al. Demonstration of a state-insensitive, compensated nanofiber trap. *Phys. Rev. Lett.*, **109**, 033603 (2012).

³⁶Vetsch, E., et al. Optical interface created by laser-cooled atoms trapped in the evanescent field surrounding an optical nanofiber. *Phys. Rev. Lett.*, **104**, 203603 (2010).

³⁷Boller, K. J., et al. Observation of electromagnetically induced transparency. *Phys. Rev. Lett.*, **66**, 2593 (1991).

³⁸Geng, J., et al. Electromagnetically induced transparency and four-wave mixing in a cold atomic ensemble with large optical depth. *New. J. Phys.*, **16**, 113053 (2014).

³⁹Ding, D. S., et al. Optical precursor with four-wave mixing and storage based on a cold-atom ensemble. *Phys. Rev. Lett.*, **114**, 093601 (2015).

⁴⁰Gulati, G. K., et al. Polarization entanglement and quantum beats of photon pairs from four-wave mixing in a cold ^{87}Rb ensemble. *New J. Phys.*, **17**, 093034 (2015).

⁴¹Meltz, G., Morey, W. & Glenn, W. Formation of Bragg gratings in optical fibers by a transverse holographic method. *Opt. Lett.*, **14**, 823 (1989).

⁴²Kato, S., & Aoki, T. Strong Coupling between a Trapped Single Atom and an All-Fiber Cavity. *Phys. Rev. Lett.*, **115**, 093603 (2015).

⁴³Kimble, H. Strong Interactions of Single Atoms and Photons in Cavity QED. *Phys. Scr.*, **127**, T76 (1998).

ACKNOWLEDGMENTS

The authors would like to thank E. Haller, K. Poulios, P. Verlot, G. Buonaiuto and the ErBeStA team for useful discussions. This project was supported by the EPSRC grants EP/R024111/1, EP/K023624/1, EP/M013294/1 and by the European Commission grants QuILMI (no. 295293) and ErBeStA (no. 800942). We acknowledge support from the University of Nottingham through a Birmingham-Nottingham collaboration grant.

V. AUTHOR CONTRIBUTIONS

L.H. conceived the experiments and oversaw the work. System construction and testing was commenced by J.N. and N.C. and completed by N.C. and E.D.R.. E.D.R. conducted the experiment and collected the published data, with assistance from N.C.. E.D.R. and N.C. wrote the paper with assistance from L.H.. All authors contributed to the manuscript.